What Limits Zonal Flow Shears in (nearly) Collisionless Drift-Wave Turbulence?

T. Zhang[1], R.A. Heinonen[1,2], and P.H. Diamond[1]
Department of Physics, UCSD[1] and University of Rome, Italy[2]
Supported by US D.O.E under Grant No. DE-FG02-04ER54738

*Note that bracketed numbers, like [1], indicate sources, which will be shown at the end

Introduction

- Drift wave - zonal flow turbulence is self-regulating and frequently thought of as a predator-prey system [6]
- Zonal shear feedback on the prey (drift wave) is central to transport regulation
- Simplest models have collisional friction damp the zonal flow or regulate the zonal energy
- Predator-prey model between zonal flows and drift waves: [3, 4, 10]:

$$\partial_t N = \gamma N - \alpha E_V N - \Delta\omega N^2$$

$$\partial_t E_V = \alpha N E_V - \nu_F E_V - \gamma_{nl}(N, E_V) E_V * E_V$$

α - shearing efficiency, γ - drift wave growth rate
N - turbulence energy, E_V - zonal flow energy
ν_F - frictional zonal flow damping
$\Delta\omega$ - non-linear drift wave damping
γ_{nl} - non-linear zonal flow damping

- With $\gamma_{nl} = 0$, two fixed points appear:

No Flow: $E_V = 0$ and $N = \frac{\gamma}{\Delta\omega}$ Flow: $E_V = \frac{\alpha\gamma - \Delta\omega\nu_F}{\alpha^2}$ and $N = \frac{\nu_F}{\alpha}$

- $\nu_F \to 0$ is akin to a Dimits Shift Regime ($E_{ZonalFlow} >> E_{DriftWave}$)
- Identifies the problem of collisionless saturation $\to$ what else limits E_{ZF} ?
- Tertiary instabilities like K-H $\to$ zonal flow instability?!

Critical Questions

- What regulates zonal flow stability?
- What is the stability criterion and what is the impact of zonal flow instability on DW-ZF turbulence?
- Does gradient of the mean potential vorticity ($\nabla\langle PV\rangle = \nabla(\langle n\rangle - \langle\nabla_\perp^2\phi\rangle)$) indicate zonal flow instability?
- How does the profile of the potential vorticity correlate with saturated turbulence levels?
- How does zonal flow marginality correlate with turbulence levels and what are the implications?
- Does $\mathrm{R} = \frac{E_{ZonalFlow}}{E_{DriftWave}}$ show a correlation with the profile of mean potential vorticity (PV) and zonal flow stability?

Outline

- Tested viability of $\nabla(\langle PV \rangle)$ to measure zonal flow instability by comparing to $R = \frac{E_{ZF}}{E_{DW}}$ with varying frictional damping

- **Hypothesis: $|\nabla(\langle PV \rangle)| > 0$ tends to have R > 1; $R \to 0$ has $\nabla(\langle PV \rangle) \to 0$**

- Utilized Hasegawa-Wakatani model simulations without magnetic shear (one value of $k_{||}$) to produce necessary profiles

- Goal: Quantify the relation between zonal flow stability criterion and turbulence levels and develop a model of γ_{nl}

Hasegawa-Wakatani Model

$$\partial_t \nabla_\perp^2 \phi + \{\phi, \nabla_\perp^2 \phi\} = \alpha(\phi - n) - \mu \nabla_\perp^2 \phi - \nu \nabla_\perp^6 \phi \rightarrow \partial_t \langle \nabla_\perp^2 \phi \rangle - \partial_x \langle (\nabla_\perp^2 \phi \partial_y \phi) \rangle = -\mu \langle \nabla_\perp^2 \phi \rangle \; [1,9]$$

$$\partial_t n + \{\phi, n\} = \alpha(\phi - n) - \kappa \partial_y \phi - D \nabla_\perp^4 n \rightarrow \partial_t \langle n \rangle - \partial_x \langle (n \partial_y \phi) \rangle = -D \langle \nabla_\perp^4 n \rangle$$

$\phi = \langle \phi \rangle + \tilde{\phi}$ and $n = \langle n \rangle + \tilde{n}$

$\alpha (= 2 = \frac{k_{||}^2 V_{Th}^2}{\omega \nu})$ - adiabatic operator

$\kappa (= 3)$ - density gradient drive

μ - flow-damping parameter, $\mu << \omega$

ν - hyper-viscosity constant

D - hyper-diffusive constant

- Zonal Flow Energy $= E_{ZF} = \int \int |\langle \nabla_\perp \phi \rangle|^2 dxdy$ for $\alpha > 1$
- Drift Wave Energy $= E_{DW} = \int \int |\tilde{n}|^2 + |\nabla_\perp \tilde{\phi}|^2 dxdy \simeq \int \int |\tilde{\phi}|^2 + |\nabla_\perp \tilde{\phi}|^2 dxdy$ for $\alpha > 1$
- R $= \frac{E_{ZF}}{E_{DW}}$ calculated in a 9 x 9 region selected from the simulation space
- No magnetic shear (only one value of $k_{||}$) and $\nabla \langle n \rangle$ is frozen

Rayleigh-Kuo Criterion I

- For an invisicid, incompressible 2D fluid, the Rayleigh inflection point theorem has classically been used as a necessary condition for instability within the shear flow [7].
- Derived from Euler's fluid equations, states that it is necessary for $\nabla(vorticity) = 0$ to have shear flow instability
- Rayleigh's Equation: $(U - c)(\phi'' - k^2\phi) - U''\phi = 0$ with $U(x)$ as the shear flow velocity, $\phi(x)$ is an amplitude, k as the wavenumber and c as the velocity of the infinitesimal disturbances [2]
- Rayleigh from this equation showed that $U_{xx} \rightarrow 0$, inflection point must be located in the shear flow for instability to occur
- $\alpha > 1 \rightarrow k_{||}V_{Th} > \omega$ so the Hasegawa-Mima must be used to derive a stability criterion rather than Euler's equations in the 2D fluid case
- Rayleigh-Kuo criterion, which has $\nabla(\langle PV \rangle) = \nabla(\langle n \rangle - \langle \nabla^2\phi \rangle) = 0$ [8]
- $\nabla\langle n \rangle$ constant in our simulations, setting constraint on the flow's stability $\rightarrow$ understand the flow evolution and impact on turbulence

Rayleigh-Kuo Criterion II - Derivation

$$\partial_t[(\rho_s^2\nabla^2 - 1)\tilde{\phi}] + \langle v\rangle\cdot\nabla[(\rho_s^2\nabla^2 - 1)\tilde{\phi}] + \tilde{v}\cdot\nabla(\langle n\rangle - \langle\nabla^2\phi\rangle) = 0$$

- Using the HM equation above with proper normalization and letting $\zeta = \langle n\rangle - \langle\nabla_x^2\phi\rangle + \tilde{\zeta}$, and $\tilde{\zeta} = \tilde{\phi} - \nabla_x^2\tilde{\phi}$,

$$\partial_t\tilde{\zeta} + \{\phi, \zeta\} = 0$$

Letting $\tilde{\phi} = \varphi(x)e^{(ik_y y - i\omega t)}$ with k_y real and ω complex ($\omega = \omega_r + i\omega_i$), we get

$$(\partial_x^2 - k_y^2 - 1 - (\frac{\partial_x\langle\zeta\rangle}{-\partial_x\langle\phi\rangle - \frac{w}{k_y}}))\varphi = 0$$

Multiplying by φ^* and integrating the imaginary part of our equation for x from 0 to L,

$$\frac{\omega_i}{k_y}\int_0^L \frac{\partial_x\langle\zeta\rangle}{|-\partial_x\langle\phi\rangle - \frac{w}{k_y}|^2}|\varphi|^2 = 0$$

$$\boxed{\partial_x\langle\zeta\rangle = 0 \rightarrow \partial_x(\langle n\rangle - \nabla_x^2\langle\phi\rangle) = 0}$$

- Rayleigh-Kuo criterion is a necessary condition: $(\nabla(\langle PV\rangle) = 0) \rightarrow$ zonal flow instability
- Fixed $\nabla\langle n\rangle \rightarrow$ R-K sets condition on the zonal vorticity profile relative to the zonal density profile
- ∇n drives turbulence, via familar drift wave instability, but also limits shear flow instability
- Rayleigh $(\nabla(vort) = 0)$ is wrong; Rayleigh-Kuo $(\nabla(\langle PV\rangle) = 0)$ is correct

Procedure

- Energies were calculated by integrating over a 9 x 9 region from a time-averaged BOUT++ simulation (512 x 512) as seen in Figure 1
- Changing the integration limits for evaluating the energies didn't change the overall trend in our diagrams.
  - Tested with 5x5, 7x7, and 9x9 regions, all of which showed similar results
- Simulations have constant linear density gradient drive and $\alpha = 2$
- Points are arbitrary selected to ensure impartial analysis of simulation space
  - Points near simulation border removed, as border cells are constrained by boundary conditions
- Does $\nabla(\langle PV \rangle)$ have any observable effect on R?

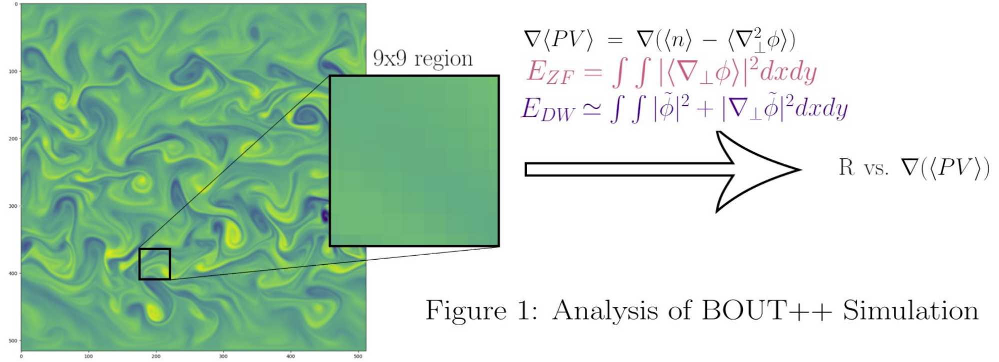

Figure 1: Analysis of BOUT++ Simulation

Results I - ∇(PV), R, Friction

- Variance in $R = \frac{E_{ZF}}{E_{DW}}$ and $\nabla(\langle PV \rangle)$ larger for lower μ
  - Less restriction on flow configuration
- Weaker damping produces a wider range of $\nabla(\langle PV \rangle)$ and R
- Density of points is larger for higher μ
- Maximum value for R decreases as μ increases as expected

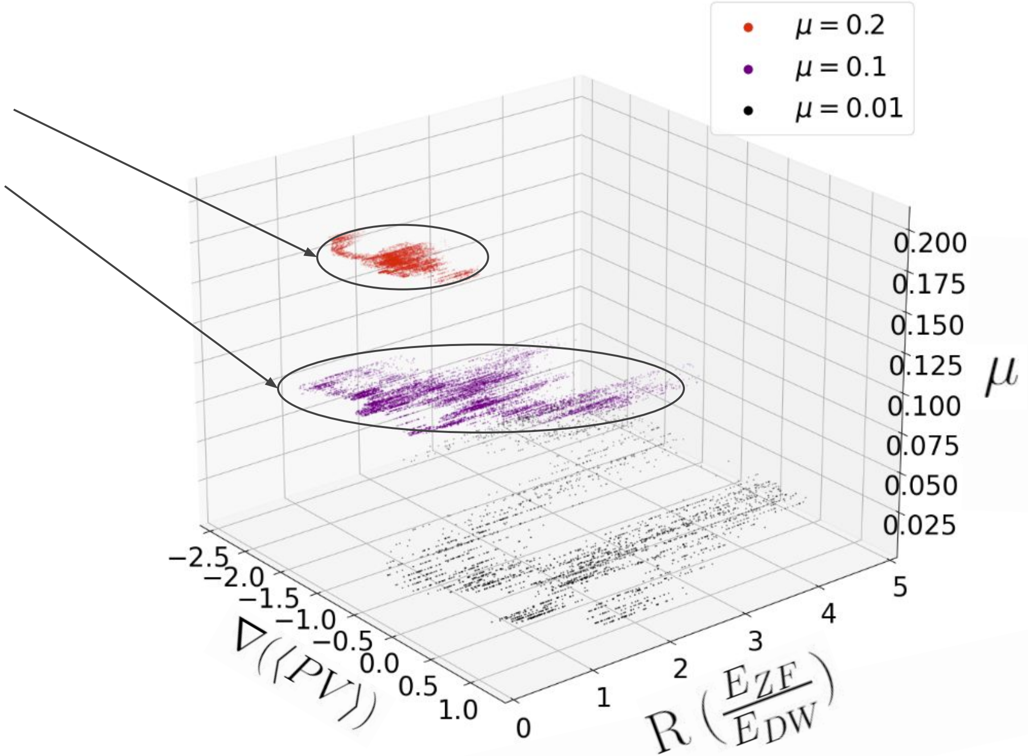

Figure 2: 3D Plot of R vs. $\nabla(\langle PV \rangle)$ vs. μ

Results II - Zonal Flow Visualization Contrast

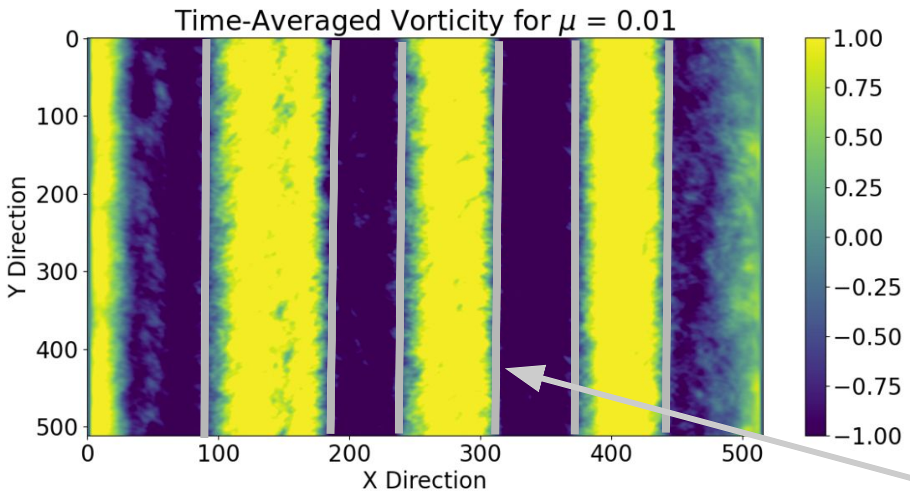

Figure 3: $\nabla(\langle PV \rangle) \neq 0$

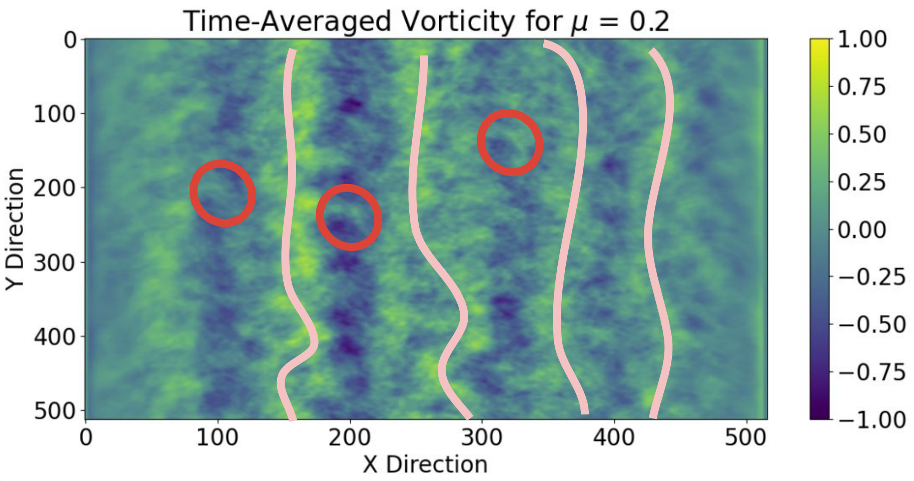

Figure 4: $\nabla(\langle PV \rangle) \to 0$

- For $\nabla(\langle PV \rangle) \neq 0$, we recover clear zonal flows as seen in Figure 3, boxed in gray
- $\nabla(\langle PV \rangle) \to 0$ has distorted zonal flows, as shown in Figure 4
- Speculate zonal flow appears to be near marginal, as jet structure can still discerned, as seen in Figure 4, highlighted in pink.
- Several re-connection and zigzag events can be seen in Figure 4, highlighted in red

Results III - Distributions For μ = 0.01

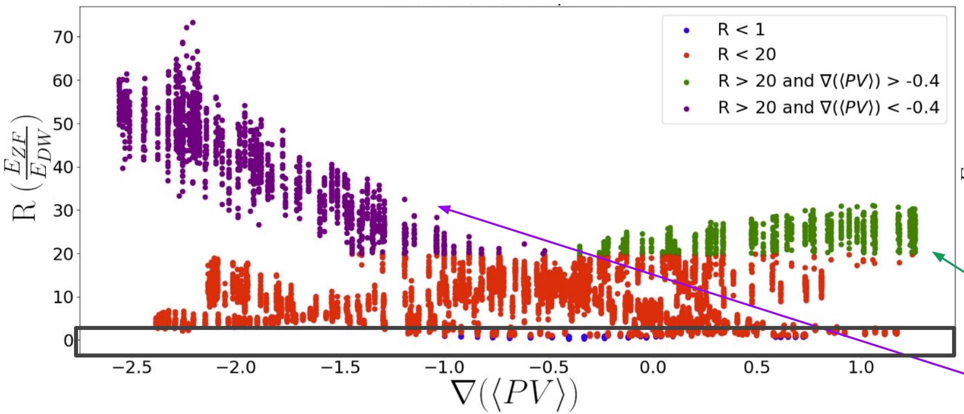

Figure 5: Distribution of R vs. $\nabla(\langle PV \rangle)$ for $\mu = 0.01$

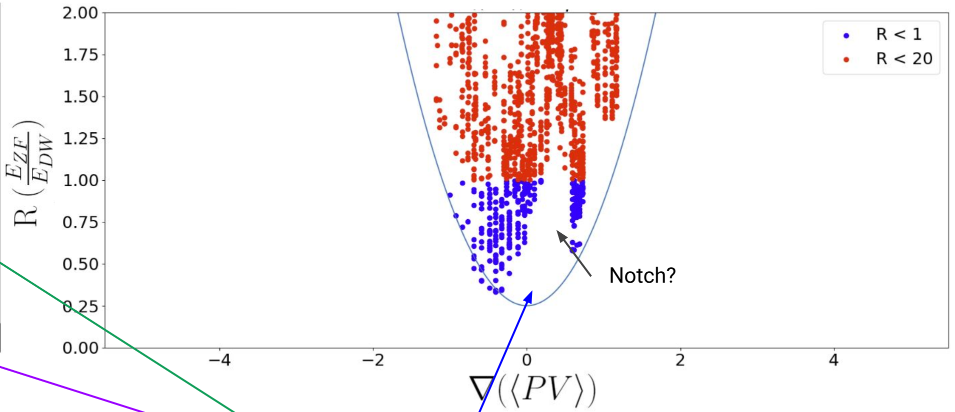

Figure 6: Distribution of R vs. $\nabla(\langle PV \rangle)$ for $\mu = 0.01$ (limited to R = 2 for viewing purposes)

- Clear persistent zonal energy dominated regime (reminiscent of Dimits), indicated by green and purple in Figure 5
- Can see that there is a centralization around $\nabla(\langle PV \rangle) = 0$
- Points with $R < 1$ also have $\nabla(\langle PV \rangle) \to 0$ as shown in Figure 6 with the blue parabola, consistent with R-K

Results IV - Distributions For μ = 0.2

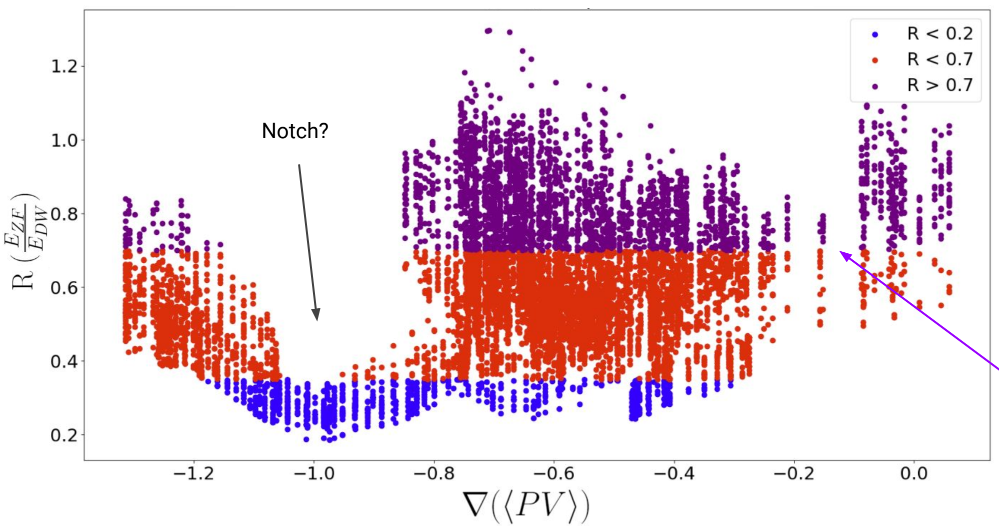

Figure 7: Distribution of R vs. $\nabla(\langle PV \rangle)$ for $\mu = 0.2$

- No clustering around $\nabla(\langle PV \rangle) \to 0$ like for lower damping as shown in Figure 7
- Suggests that higher zonal flow damping (μ) has greater effect on zonal flow stability than R-K
- Majority of points have less zonal flow energy than drift wave energy, consistent with the distorted zonal vorticity figure shown earlier
- Purple points typically have $|\nabla(\langle PV \rangle)| > 0$, with R > 0.7, also consistent with R-K
- No clear division between stable and marginally stable points.

Results V - Comparison Between Larger and Lower Damping

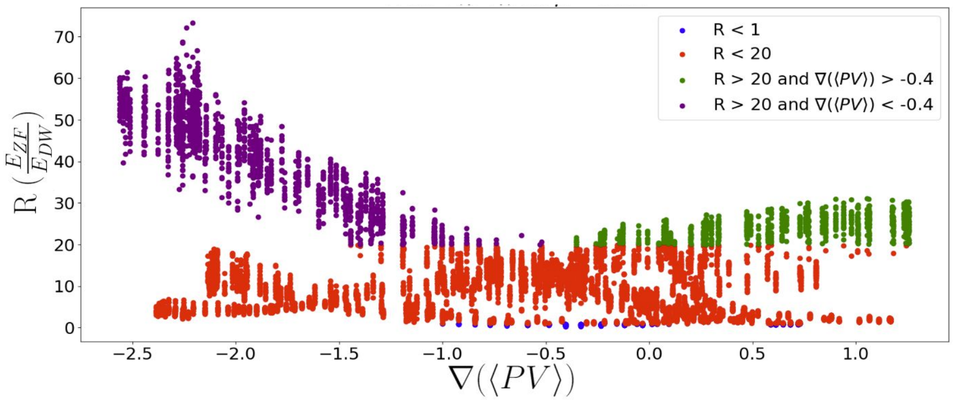

Figure 5: Distribution of R vs. $\nabla(\langle PV \rangle)$ for $\mu = 0.01$

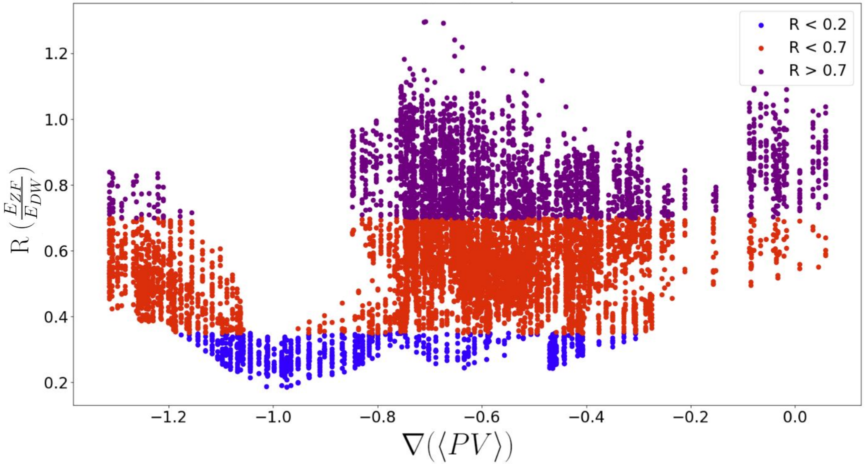

Figure 7: Distribution of R vs. $\nabla(\langle PV \rangle)$ for $\mu = 0.2$

- More zonal flow energy evident in lower damping conditions, as expected
  - Results in a higher maximum value for R
- Lower damping scenario consistent with R-K, larger damping isn't $\rightarrow$ μ directly affects R
- Dimits-like regime isn't apparent for higher damping, as expected

Comments on Analysis

- Decreasing μ usually increases maximum value of R

- $\nabla(\langle PV \rangle)$ appears to correlate well with R ($\frac{E_{ZF}}{E_{DW}}$) for low damping, $R \to 0$ has $\nabla(\langle PV \rangle) \to 0$ and $|\nabla(\langle PV \rangle)| > 0$ also has R > 20 which is consistent with R-K

- Higher damping seems to weaken the $\nabla(\langle PV \rangle) \leftrightarrow R < 1$ links, implying that μ affects R directly

Key Results

$\nabla\langle n\rangle$ is frozen

- R-K is correct, not Rayleigh
- Combination of R-K and μ define turbulent states of a system
- $\mu = 0.01$ setting $\rightarrow E_{ZF} >> E_{DW}$ states persist
- $\mu = 0.2$ setting has less zonal flow energy than $\mu = 0.01 \rightarrow$ zonal flow only marginally stable
- R vs. $\nabla(\langle PV\rangle)$ for $\mu = 0.01$ consistent with R-K
- R vs. $\nabla(\langle PV\rangle)$ for $\mu = 0.2$ not consistent with R-K, suggests that R-K isn't the dominant physics

Next Steps

- $\frac{\nabla\langle n\rangle}{n}$ scan $\rightarrow$ explore resilience of large R (Dimits-like) states
  - $\nabla\langle n\rangle$ $\rightarrow$ drives turbulence via DW mechanism
  - $\nabla\langle n\rangle$ $\rightarrow$ maintains ZF stability via R-K criterion
- $\langle n\rangle$ evolution $\rightarrow$ staircase?
- What maintains strong shearing structure?
- Suspect steep $\frac{\nabla\langle n\rangle}{n}$ via R-K!
- Physics and form of $\gamma_{nl}(N, E_V)$

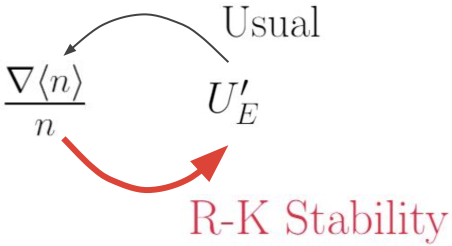

Rayleigh unstable!
(But R-K?)

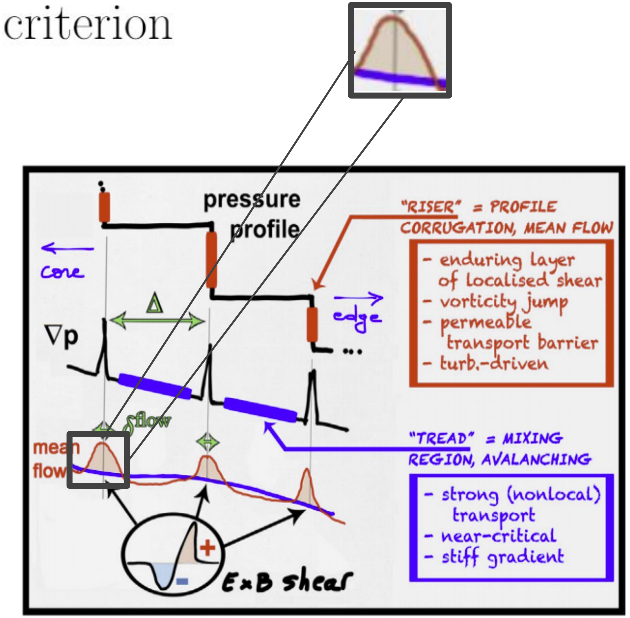

Figure 8: Staircase in Vorticity [5]

References I

[1] Akira Hasegawa and Masahiro Wakatani, "Self-Organization of Electrostatic Turbulence in a Cylindrical Plasma", Physical Review Letters, 59 (14), 1987.

[2] Balmforth, N. J., and P. J. Morrison. "A necessary and sufficient instability condition for inviscid shear flow." Studies in Applied Mathematics 102.3 (1999): 309-344.

[3] Diamond, P., Liang, Y.M., Carreras, B., & Terry, P. (1994). Self-Regulating Shear Flow Turbulence: A Paradigm for the L to H Transition. Phys. Rev. Lett., 72, 2565–2568.

[4] Fujisawa, A. (2008). A review of zonal flow experiments. Nuclear Fusion, 49, 013001.

[5] G. Dif-Pradalier, G. Hornung, X. Garbet, Ph. Ghendrih, V. Grandgirard, G. Latu, & Y. Sarazin (2017). The E x B staircase of magnetised plasmas. Nuclear Fusion, 57(6), 066026.

[6] Gurcan, O., & Diamond, P. (2015). Zonal flows and pattern formation. Journal of Physics A, 48(29), 293001.

References II

[7] J. W. S. Rayleigh. On the stability or instability of certain fluid motions, Proc. Lond. Math. Soc. 9: 57–70 (1880).

[8] H.-L. Kuo, J. Meteor. 6, 105 (1949).

[9] Numata, R., Ball, R., & Dewar, R. (2007). Bifurcation in electrostatic resistive drift wave turbulence. Physics of Plasmas, 14(10), 102312.

[10] Schmitz, L., Zeng, L., Rhodes, T., Hillesheim, J., Peebles, W., Groebner, R., Burrell, K., McKee, G., Yan, Z., Tynan, G., Diamond, P., Boedo, J., Doyle, E., Grierson, B., Chrystal, C., Austin, M., Solomon, W., & Wang, G. (2014). The role of zonal flows and predator–prey oscillations in triggering the formation of edge and core transport barriers. Nuclear Fusion, 54(7).

[11] Zhu, H., Zhou, Y., & Dodin, I. (2018). On the Rayleigh–Kuo criterion for the tertiary instability of zonal flows. Physics of Plasmas, 25(8), 082121.

Thank you for your attention!

Additional Graphs + Tables I

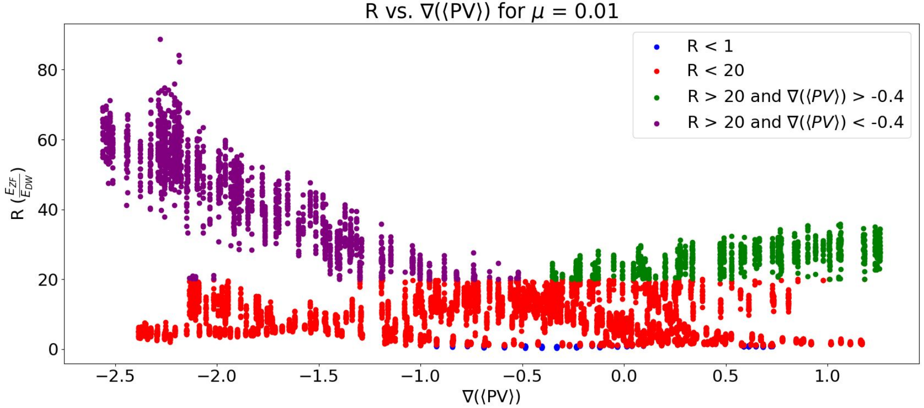

Figure 9: 5 x 5 Integration Region

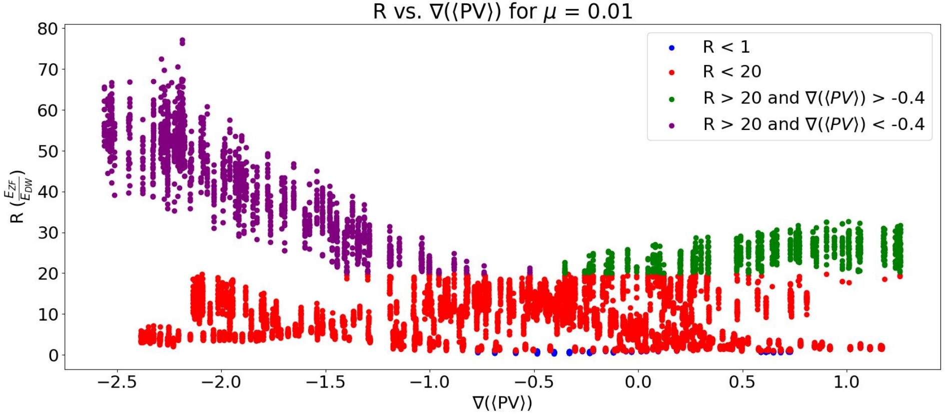

Figure 10: 7 x 7 Integration Region

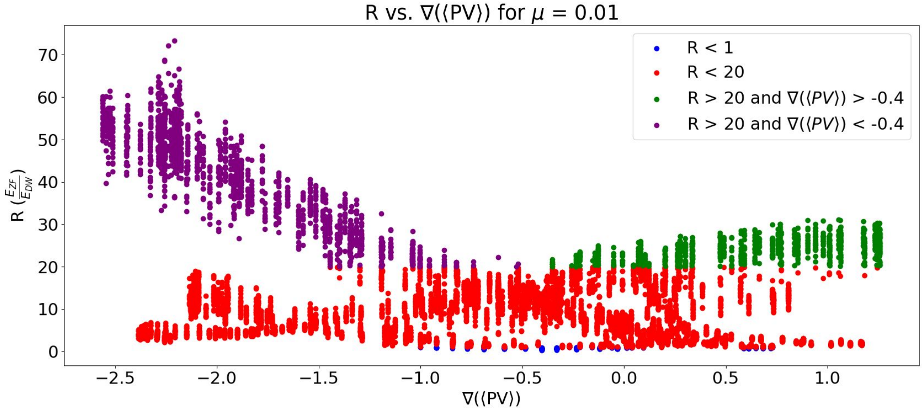

Figure 11: 9 x 9 Integration Region

Additional Graphs + Tables II

μ	Variance in ∇ (PV)	Variance in R
0.01	1.02	198.04
0.1	0.21	0.43
0.2	0.08	0.03

Table 1: Variances for Varying Frictional Damping

Additional Graphs + Tables III

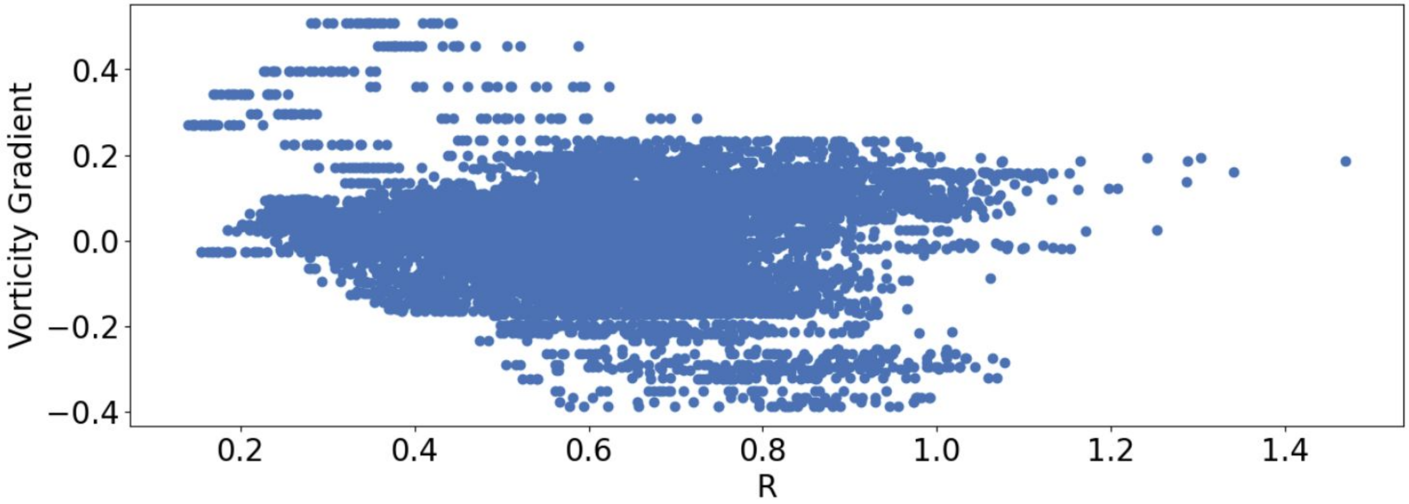

Figure 12: Distribution of R vs. Zonal Flow Gradient for μ = 0.2